Discovery of Novel Small-Molecule Inhibitors of Human Epidermal Growth Factor Receptor-2: Combined Ligand and Target-Based Approach

Rambabu Gundla,[†] Roza Kazemi,[†] Ramadevi Sanam,[‡] Ravikumar Muttineni,[‡] Jagarlapudi A. R. P. Sarma,[‡] Raveendra Dayam,[†] and Nouri Neamati*,[†]

Department of Pharmacology and Pharmaceutical Sciences, University of Southern California, School of Pharmacy, 1985 Zonal Avenue, Los Angeles, California, Division of Informatics, GVK Biosciences Pvt. Ltd., Technocrats Industrial Estate, Balanagar, Hyderabad, Andhra Pradesh, India

Received November 5, 2007

Consensus virtual screening models were generated and validated utilizing a set of known human epidermal growth factor receptor-2 (HER2) inhibitors and modeled HER2 active and inactive state structures. The virtual screening models were successfully employed to discover a set of structurally diverse compounds with growth inhibitory activity against HER2-overexpressing SKBR3 breast cancer cell line. A search of a 3D database containing 350000 small-molecules using the consensus models retrieved 531 potential hits. Of the 531 hits, 57 were selected for testing in SKBR3 cells on the basis of structural novelty and desirable drug-like properties. Seven compounds inhibited growth of SKBR3 cells with IC_{50} values <10 μM. These lead compounds have desirable physicochemical properties and are excellent candidates for further optimization.

Introduction

The human epidermal growth factor receptor-2 (HER2) proto-oncogene encodes a 185 kDa glycoprotein that plays a key role in breast cancer. The HER tyrosine kinase receptor family comprises four homologous epidermal growth factor (EGF) receptors: EGFR/ErbB1/HER1, HER2/Neu/ErbB2, HER3/ErbB3, and HER4/ErbB4[a]. The HER family of receptors are among the most studied cell signaling families in cancer biology.[1] Each protein has an extracellular ligand-binding domain, a transmembrane region, and an intracellular cytoplasmic domain.[2] The extracellular domain is involved in recognizing and binding ligands that activate the receptor. The cytoplasmic domain contains a tyrosine kinase region and a carboxy terminal tail that harbors tyrosine autophosphorylation sites. The HER family of receptors have similar structures and a high degree of homology in the tyrosine kinase region, although they possess diverse characteristics that determine their signaling specificity. The tyrosine kinase domains of HER2 and HER4 show approximately 80% homology to that of HER1, whereas HER3 lacks intrinsic tyrosine kinase activity.[3] The extracellular domains are less conserved among the four receptors, which is indicative of different specificity in ligand binding.

The HER receptors exist as inactive monomers. A variety of ligands can bind to the extracellular domains of HER1, HER3, and HER4 and activate these receptors. These ligands have different specificities for each receptor, resulting in different cellular signaling affects.[4] There is no known ligand for HER2, rendering it an orphan receptor. Upon binding to ligands, the extracellular domains of HER1, HER3, and HER4 receptors undergo conformational changes that allow activation of the receptors by either a homodimerization or a heterdimerization process. The dimerization process is essential to stimulate the tyrosine kinase activity of the receptors for subsequent generation of an intracellular signal. Interestingly, constitutive conformation of the extracellular domain of the orphan receptor HER2 resembles the conformation of ligand activated extracellular domains of the other HER receptors. This autoactivated conformation enables HER2 to perform as a preferred dimerization partner for all other HER receptors.[5,6]

In a variety of human cancer cells, aberrant signaling involving HER receptors stimulate pathways that activate many of the properties associated with cancer, including proliferation, migration, metastasis, angiogenesis, and resistance to apoptosis. Because of the high frequency of abnormalities in receptor signaling in human cancers, the HER family is an attractive target for therapeutic development. The frequently observed causes of signaling abnormalities in cancers involving HER receptors are overexpression of receptors, overproduction of growth factor ligands, and ligand-independent receptor activation. The HER receptors are overexpressed or deregulated in a wide variety of cancers including breast, colorectal, ovarian, prostate, and nonsmall cell lung cancers. Importantly, overexpression of HER receptors is associated with poor disease prognosis and reduced survival. Mounting preclinical and clinical evidence supports the rationale behind the HER family targeted anticancer therapeutic approaches. Although the complexities of the signaling pathways involving the HER family of receptors are not fully understood, several possible points within the pathways have been identified to be therapeutically advantageous if interrupted.[7] Drugs targeting HER family fall into three main categories depending on the receptor region targeted: extracellular, intracellular, and nuclear. The most promising and advanced therapeutic strategies targeting HER receptors are monoclonal antibodies and small-molecule tyrosine kinase inhibitors. Intensive research over the last 20 years in these areas has yielded a number of promising anticancer therapeutics. Currently, five anticancer therapeutics targeting the HER receptor family have been approved. Two of them are humanized antibodies, trastuzumab (Herceptin) and cetuximab (Erbitux), targeted to the extracellular domains of HER2 and HER1, respectively. The remaining three are small-molecule

* To whom correspondence should be addressed. Phone: 323-442-2341. Fax: 323-442-1390. E-mail: neamati@usc.edu.

[†] Department of Pharmacology and Pharmaceutical Sciences, University of Southern California, School of Pharmacy.

[‡] Division of Informatics, GVK Biosciences Pvt. Ltd.

[a] Abbreviations: HBA, hydrogen bond acceptor; HBD, Hydrogen bond donor; HRA, hydrophobic aromatic; rmsd, root-mean-square deviations; GOLD, genetic optimization for ligand docking; OFF, open force field; EGF, epidermal growth factor

10.1021/jm7013875 CCC: $40.75
Published on Web 05/24/2008

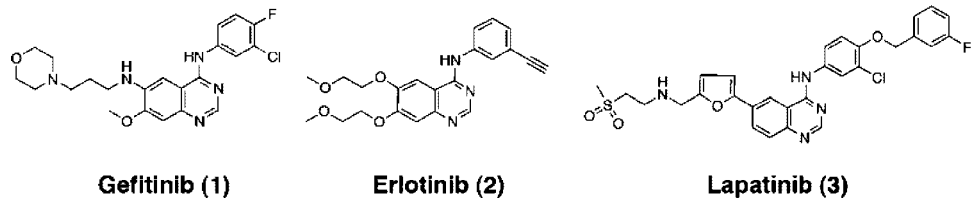

Figure 1. Clinically used HER family targeted kinase inhibitors.

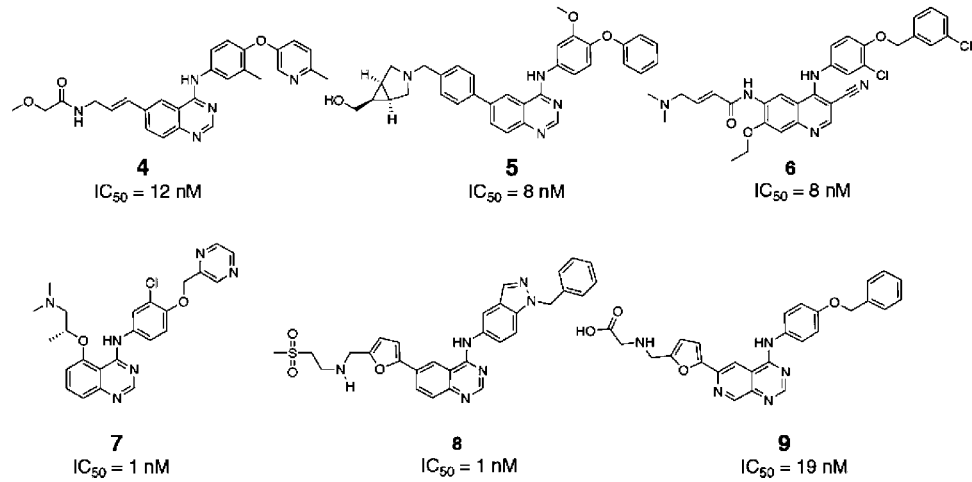

Figure 2. Training set compounds (**4**−**9**) used to generate qualitative pharmacophore models.

tyrosine kinase inhibitors. Gefitinib (**1**) and Erlotinib (**2**) are targeted to the HER1 tyrosine kinase domain, and Lapatinib (**3**) is targeted to the HER2 tyrosine kinase domain[8] (Figure 1). Several small-molecule HER tyrosine kinase inhibitors are being investigated in various stages of clinical trials.[9,10] These compounds compete with ATP for binding to the ATP site on the receptor's intracellular tyrosine kinase domain. Through binding the ATP site and inhibiting catalytic activity, they block autophosphorylation of key tyrosine residues on the receptor kinase domain. This phosphorylation block disrupts activation of receptor mediated downstream signaling cascades. The enormous progress in the discovery of anticancer therapeutics targeting the HER receptor family coupled with the success of small-molecule inhibitors targeting the intracellular HER2 domain make this approach very promising for the treatment of HER2 mediated cancers. These molecules act by binding either reversibly or irreversibly to the C-terminal tyrosine kinase domain of HER2, thereby inhibiting autophosphorylation of the receptor. Here, we used computational methods to discover small molecule inhibitors targeted to the C-terminal tyrosine kinase domain of HER2.

Application of computational methodologies in the drug discovery process is well established. Other technologies, including combinatorial chemistry and high-throughput screening (HTS), are also being used to synthesize and screen large numbers of compounds in a short period of time to boost the productivity of the drug discovery process. Several virtual screening techniques are currently available to rapidly screen compounds from virtual compound databases. In virtual screening, computational models are used to predict the biological activity of compounds. The computational models can be generated and validated utilizing either the 3D structure of the target or a set of active analogues specific to the target. Computational models can also be built combining information from structure of the drug target and a set of active analogues specific to the target.[11] Utilizing these technologies to discover small-molecule HER2 inhibitors, we employed consensus models generated by combining both receptor structure and active analogue-based methods. In this study, we present the pharmacophore modeling, the homology modeling of active and inactive states of HER2 structure, and finally the use of these models to discover a set of novel HER2 inhibitors with activity in HER2-overexpressing SKBR3 cells.

Results and Discussion

Pharmacophore Models. The best common feature pharmacophore model indicated the importance of H-bond acceptor (HBA), H-bond donor (HBD), and hydrophobic aromatic (HRA) features, which were further confirmed in the quantitative models. Several quantitative models were generated utilizing the training set (**3**, **7**−**27**) along with HER2 inhibitory activities (Figures 2, 3 and Table 1). The top ten hypotheses were composed of HBA, HBD, and HRA features. The values of ten hypotheses such as cost, correlation (r), and root-mean-square deviations (rmsd) are statistically significant (Table 2). In addition to an estimation of activity of the training set molecules, the pharmacophore model should also accurately predict activity of the test set molecules. Two statistical methods were employed to rank the ten resultant hypotheses. In the first method, all ten hypotheses were evaluated using a test set of 452 known HER2 inhibitors, which are not included in the training set. These molecules cover a wide range of HER2 inhibitory activity (3−9-fold). Predicted activities of the test set were calculated using all ten hypotheses and correlated with experimental activities. Of the ten hypotheses, Hypo5 showed a better correlation coefficient compared to the other nine hypotheses. A second statistical test includes calculation of false positives, false negatives, enrichment, and goodness of hit to determine robustness of hypotheses. Under all validation conditions, Hypo5 performed superior as compared to the other nine hypotheses (Figure 4A).

Hypo5 demonstrated excellent prediction of HER2 inhibitory activities of the training set compounds (Table 1). All six highly active compounds of the training set were correctly predicted

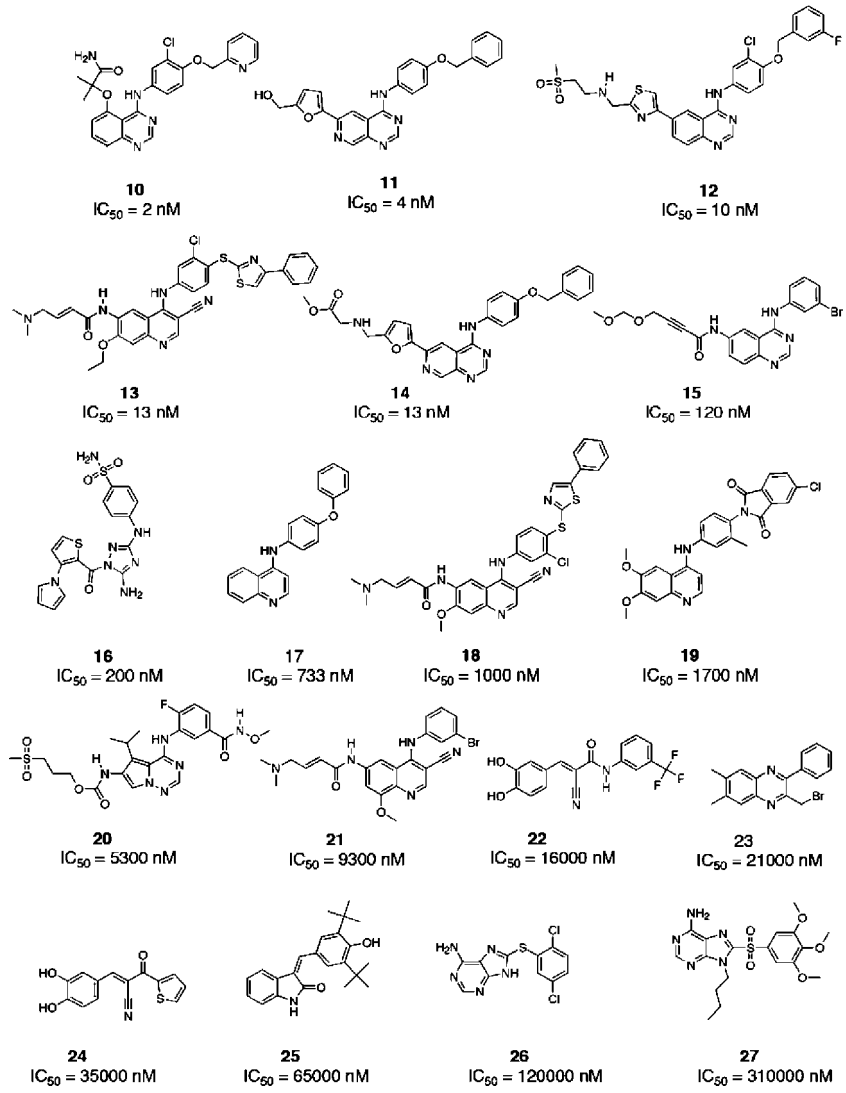

Figure 3. Training set compounds (**10**−**27**) used to generate quantitative pharmacophore models.

Table 1. Hypo5 Predicted Activities of the Training Set Compounds (**3**, **7**−**27**)

compound	experimental (IC_{50}, nM)	predicted (IC_{50}, nM)	fit value
3	9	5.7	8.91
7	1	1.5	9.49
8	1	1.4	9.51
9	19	6.7	8.84
10	2	3	9.20
11	4	7.5	8.79
12	10	8.7	8.73
13	13	47	7.99
14	13	14	8.51
15	120	270	7.24
16	200	180	7.42
17	733	190	7.28
18	1000	380	7.09
19	1700	3990	6.69
20	5300	1800	6.40
21	9300	3900	6.08
22	16000	38000	5.09
23	21000	89000	4.72
24	35000	47000	5.00
25	65000	53000	4.95
26	120000	71000	4.82
27	310000	40000	5.06

as highly active. Of the seven moderately active compounds, six were predicted as moderately active, while one compound was predicted to be highly active. All nine inactive compounds of the training set were predicted as inactive. Activities of the compounds were not only correctly predicted, but the fit values also confer a good measure of how well the pharmacophoric features of Hypo5 were mapped onto the chemical features of the compounds. All features of Hypo5 (HBA, HBD, and three HRA) were mapped onto the highly active compounds of the training set (Figure 4B). One or more features of Hypo5 were partially mapped onto the moderately active compounds of the training set (Figure 4C). Many of the inactive compounds in the training set did not map onto one or more features of Hypo 5 (see for example compound **20** in Figure 4D).

Hypo5 was used to search the test set of known HER2 inhibitors. Database mining was performed using the BEST flexible searching technique. The results were analyzed using a set of parameters such as hit list (H_t), number of active percent of yields (*%Y*), percent ratio of actives in the hit list (*%A*), enrichment factor (*E*), false negatives, false positives, and goodness of hit score (GH) (Table 3). Hypo 5 succeeded in the retrieval of ∼72% of the active compounds from the test set. In addition, the pharmacophore also retrieved 64 inactive compounds (false positives). It predicted 55 active compounds as inactive (false negatives). An enrichment factor of 1.67 and a GH score of 0.536 indicate the quality of the model. Overall, a strong correlation was observed between the Hypo5 predicted activity and the experimental HER2 inhibitory activity (pIC_{50}) of

Table 2. Analysis of Pharmacophore Models Generated by Hypogen Algorithm

hypo	total cost	cost difference[a]	error cost	rms deviation	training set	feature[b]
1	78.639	80.301	62.598	0.798	0.973	ADRR
2	79.722	79.218	63.796	0.882	0.967	ADRR
3	81.577	77.362	65.254	0.974	0.960	ADRR
4	81.636	77.303	66.339	1.037	0.953	ADRRR
5	**81.791**	**77.148**	**66.456**	**1.044**	**0.953**	**ADRRR**
6	81.874	77.065	64.108	0.902	0.966	ADRR
7	82.846	76.093	66.451	1.044	0.953	ADRR
8	83.890	75.049	67.846	1.120	0.946	ADRRR
9	85.148	73.791	69.858	1.221	0.935	ADRRR
10	86.974	71.965	68.504	1.154	0.944	ADRR

[a] (Null cost−total cost), null cost = 158.94, fixed cost = 72.47. For Hypo-5: weight = 1.169 and configuration = 14.164. [b] A: H-bond acceptor, D: H-bond donor, and R: Hydrophobic aromatic.

Table 3. Hypo5 Validation Using a Set of Known HER2 Inhibitors

parameter	value
total compounds in database (D)	452
total number of actives in database (A)	195
total hits (H_t)	204
active hits (H_a)	140
% yield of actives	68.63
% ratio of actives in the hit list	71.79
enrichment factor or enhancement (E)	1.67
false negatives	55
false positives	64
GH score (goodness of hit)[a]	0.536

[a] $GH = \{[(H_a/4H_t(A))][(3A + H_t)][(1 - ((H_t - H_a)]\}/(D-A)$. GH score of 0.6−0.7 indicates a very good model.

the training and test set compounds (Figure 6). However, the Hypo5 model has a greater tendency to show false positives. This could be attributed to high structural similarity in active and inactive HER2 inhibitors, resulting in an inability to discriminate this pattern by the pharmacophore model. We further extended this study to structure-based design and developed a consensus model to limit the number of false positive and false negative hits and to further understand the binding of inhibitors to the active site of HER2 active and inactive states.

Validation of HER2 Active and Inactive States and Docking Simulations. We constructed homology models using HER2 sequence (Figure 5) for the HER2 active and inactive state conformations to predict the binding mode of HER2 inhibitors. The 3D models of HER2 (active and inactive states) were validated by docking of Erlotinib (cocrystallized inhibitor with the active state of HER1 (1M17 PDB)) on to the HER2 active state model, and Lapatinib (cocrystallized inhibitor with the inactive state of HER1 (1XKK PDB)) on to the HER2 inactive model using GOLD v.3.2 (Genetic Optimization for Ligand Docking, Cambridge Crystallographic Data Center, Cambridge, UK).[12] The ATP binding site was defined as the active site. Analysis of the predicted binding conformations of Erlotinib and Lapatinib inside the ATP binding site of modeled HER2 active and inactive structures shows a general agreement with the hinge region interactions commonly observed in the kinase family. The key binding interactions are correlated with the established pharmacophore model. The two inhibitors showed similar pattern of interactions in the binding site of HER1 (cocrystal structures) and modeled HER2 structures (Figures 7–8). In the predicted Erlotinib binding conformation in the HER2 active state, N1 of the quinazoline accepts an N···H−N bond from the backbone NH of Met801 (Figure 7). A strong C−H···O hydrogen bond is formed between the activated C2−H group and the backbone carbonyl oxygen of Glu799. The distance between the N3 atom of the quinazoline and OH of Thr798 is 3.54 Å. Additionally, the 6- and 7-substituents project outside the active site (actually, in the cleft region between the C-terminal and N-terminal lobes). The meta-substituted 4-anilino group fits well in the hydrophobic pocket surrounded by amino acid residues Phe864, Asp863, Val797, Leu796, Met774, Ile752, Lys753, and Phe731. In the complex of modeled HER2 inactive state and Lapatinib, the N1 atom of the quinazoline is involved in an H-bonding interaction with the backbone NH of Met801 at a distance of 2.04 Å. The distance between the N3 atom of the quinazoline and OH of Thr798 is 3.39 Å. The aniline portion of the inhibitor is surrounded by residues Thr798, Lys753, Thr862, and Asp841. The 3-methoxy-1-flouro phenyl group occupies a pocket surrounded by Val797, Met774, Arg784, Ser783, Phe864, Gly865, and Leu866 (Figure 8). It was observed from the docking results that overall nature and number of interactions of inhibitors that are binding to the active sites in the active and inactive states of modeled HER2 structure are similar.[13] A second type of analysis was carried out to verify goodness of the models for virtual screening. The training set molecules (**3**, **7**−**27**) were also docked to both the active and inactive state of HER2. The docking scores of compounds across three docking procedures (GOLD v. 3.2, Glide v.3.5,[14] and eHiTS v.6.2[15]) in the HER2 active and inactive states were well correlated with the experimental (pIC_{50}) activities (Table 4). Further, the models were evaluated using a large set of the test set compounds (Table 5). All together, the predicted binding conformations and docking scores of known inhibitors validate the quality and applicability of the modeled HER2 active and inactive state structures for virtual screening studies. In addition, it was observed that docking could limit the number of false positive hits compared to Hypo5. A slight increase in the number of false negatives was observed in docking hits. Interestingly, the pharmacophore and docking models showed complementary behavior in limiting the number of false positive and false negative hits. On the basis of these observations, we designed a consensus virtual screening model by combining the pharmacophore and docking models to identify novel HER2 inhibitors.

Consensus Model. The individual screening models, either the pharmacophore or docking model, each performed adequately to separate known active and inactive HER2 inhibitors. To further enhance our models, we built a consensus model by combining analogue and structure-based methods. The equations, eqs 1 and 2, were generated for inactive and active states of HER2, respectively.

$$\text{predicted activity } (pIC_{50}) = 0.233 + 0.7104\,(\text{Pharmacophore } pIC_{50}) - 0.063\,(\text{Glide score}) + 0.013\,(\text{GOLD score}) - 0.159\,(\text{eHiTS score})$$

$$n = 158,\ r^2 = 0.846,\ q^2 = 0.684,\ F = 90.12,\ \text{PRESS} = 32.691,\ \text{and } r^2_{\text{pred}} = 0.69 \quad (1)$$

$$\text{predicted activity } (pIC_{50}) = 0.206 + 0.698\,(\text{pharmacophore } pIC_{50}) - 0.096\,(\text{Glide score}) + 0.012\,(\text{GOLD score}) - 0.127\,(\text{eHiTS score})$$

$$n = 158,\ r^2 = 0.763,\ q^2 = 0.674,\ F = 88.50,\ \text{PRESS} = 33.691,\ \text{and } r^2_{\text{pred}} = 0.66 \quad (2)$$

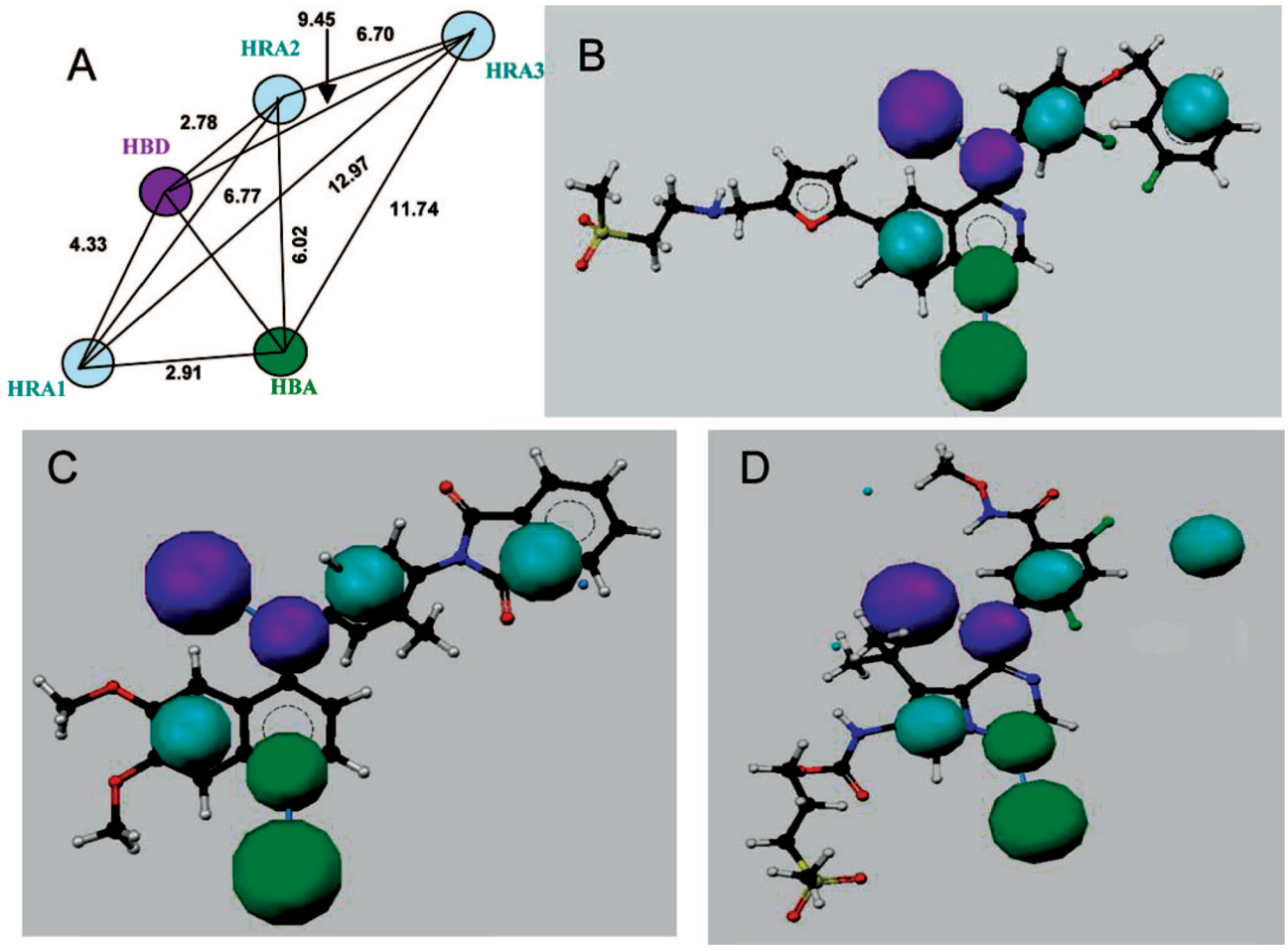

Figure 4. (A) Three-dimensional arrangement of pharmacophoric features in the quantitative pharmacophore model (Hypo5). Pharmacophore features are: H-bond acceptor (HBA) as green, hydrophobic aromatic (HRA1- HRA3) as cyan, H-bond donor (HBD) as magenta. (B) Hypo5 is mapped onto Lapatinib (**3**). (C) Mapping of Hypo5 onto a moderately active compound **14**, (D) mapping of Hypo5 onto an inactive compound **20**.

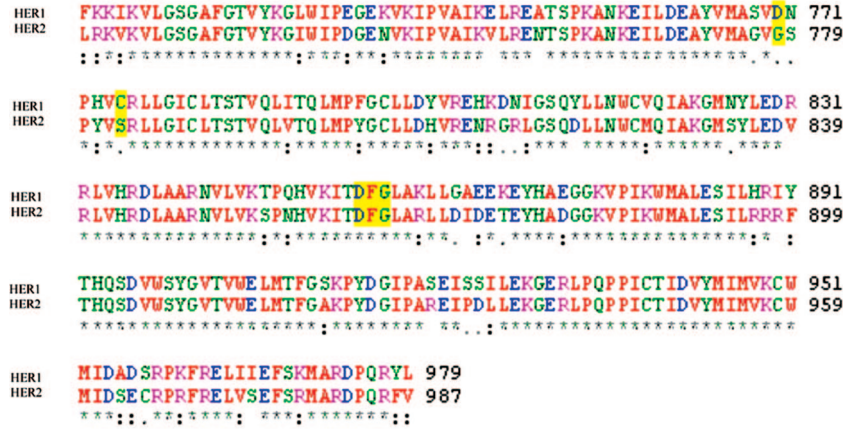

Figure 5. Alignment of the catalytic domain sequences of HER1 and HER2. Highlighted are prominent amino acid residues Asp-770, Cys-775, and the DFG motif.

Equation 1 confirms the predicted power of a consensus model obtained with docking scores of the HER2 inactive state along with pharmacophore predicted activity as proven by significant statistical relevance. Interestingly, eq 2 obtained with docking scores using the HER2 active state along with the pharmacophore predicted activity afforded a similar pattern with a good correlation compared to eq 1 (Figure 9). A significant correlation was observed between predicted activity values from consensus models of both HER2 conformational states and experimental biological activity. Further, eqs 1 and 2 were used to calculate a number of statistical parameters such as hit list (H_t), percent active (*%Y*), percent ratio of actives in the hit list (*%A*), enrichment factor of (*E*), false negatives, false positives, and goodness of hit score to cross validate the predicted power of the models (Table 6).

We observed that the consensus models significantly reduced the number of false positives and false negatives (Figure 9 and Table 6). Equations 1 and 2 show similar statistical parameters

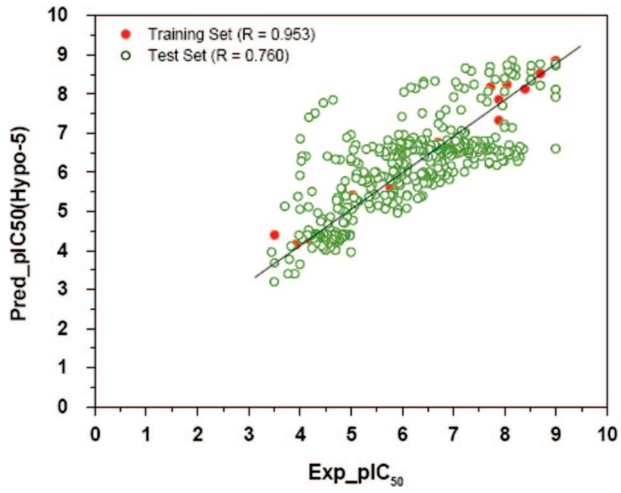

Figure 6. Scatter plot shows correlation between experimental and Hypo5 predicted activities of known HER2 inhibitors.

and suggest that a good HER2 inhibitor would have to fit with the pharmacophore and have to successfully interact with both active and inactive states of HER2. Therefore, we used these two equations to screen the compounds against HER2.

Database Screening. The Hypo5 model was used as a query to screen a database of 350000 compounds. The search retrieved 961 hits (0.27% of database). A set of 531 compounds with a predicted IC_{50} value < 1 μM were selected and docked onto the active and inactive states of HER2 using GOLD, Glide, and eHiTs. The Hypo5 predicted activity and docking scores from all three docking algorithms were substituted in to consensus eqs 1 and 2 to predict activity for the 531 pharmacophore hits. Finally, 57 hits with a predicted activity value of <100 μM were selected for an in vitro assay against the SKBR3 cell line, a HER2-overexpressing human breast cancer cell line.[16–18]

Compound Selection and Cell Growth Inhibition Assay. The compound selection process implemented is shown as a flowchart in Figure 10. Fifty-seven compounds were selected for the cytotoxicity assay in the HER2-overexpressing SKBR3 cell line. Of the 57 compounds tested, 12 compounds (21%) inhibited cell growth with an IC_{50} value ranging from 2 to 50 μM (Table 7). The tricyclic 4-anilino benzo[*g*]quinoline analogues (**28** and **29**) were the most potent among the tested compounds. Compounds **28** and **29** inhibited the proliferation of SKBR3 cells with IC_{50} values of 2 ± 0.2 and 2 ± 0.2 μM, respectively. Compounds **28** and **29** are equipotent to that of the tricyclic 3-cyanobenzo[*g*]quinolines with a 4-phenoxyanilino substitution at fourth position, which were previously reported as ATP competitive inhibitors using a panel of kinases.[19,20] It is also observed that the potency of the compounds decreases with an increasing length of the aliphatic chain between the benzo[*g*]quinolin-4-amine and phenyl group (**30**).The replacement of phenyl group of compound **30** with the 1,4-methylpiperazine led to compound **31** with a decreased inhibitory activity. Compounds **30** and **31** inhibited SKBR3 cell growth with IC_{50} values of 8 ± 0.3 and 15 ± 0.4, respectively (Table 7).

As envisaged by the pharmacophore model, the 2-methylquinoline (**32**−**33**) exhibited enhanced inhibitory activity as compared to compound **28** against the proliferation of SKBR3 cells.[21] Partial mapping of Hypo5 onto one of the tested compounds (**34**), a quinazoline analogue, illustrates that the two-carbon linker between N and the phenyl group of aniline is not required for enhanced activity. Compound **35**, containing the 4-anilino thieno[2,3-*d*]pyrimidin core, inhibited cell growth with an IC_{50} value of 9 ± 0.5 μM. The two-carbon linker containing thieno[2,3-*d*]pyrimidin analogue (**36**) inhibited the SKBR3 cell growth with an IC_{50} value of 14 ± 0.5 μM, a slightly higher value than that of compound **35** (9 ± 0.5 μM). Interestingly, compound **37**, a thieno[2,3-*d*]pyrimidine-4-thiol analogue, showed moderate inhibitory activity with an IC_{50} value of 16 ± 0.3 μM. The [1,2,4]triazolo[1,5-*a*]pyrimidin-7-amine scaffold containing compounds **38** and **39** also displayed moderate growth inhibition with IC_{50} values of 9 ± 0.5 and 14 ± 0.4 μM, respectively. These results suggest that compound **28** with a variety of substituents at C-7 and C-8 of the tricyclic moiety confers improved activity. Further chemical optimization is required to better understand key residues for activity and selectivity.

Finally, it is important to bear in mind that in general kinase inhibitors are not highly selective for their target. For example, Gleevec is known to inhibit at least 10 other kinases in nM range. Therefore, we expect that the compounds presented in this study could potentially inhibit other kinases especially, the HER family members. Detailed kinase activity profile of these compounds and their optimization derivatives are in progress in our laboratory.

Conclusions

Several structurally diverse compounds possessing growth inhibitory potency against HER2-overexpressing cancer cells were identified using consensus virtual screening models (eqs 1 and 2). The consensus models were generated and validated utilizing a set of known HER2 inhibitors. These compounds bearing amenable chemical and structural features are potential leads for drug design strategies targeting HER2. Further structural optimization to enhance their inhibitory activity is in progress and will be reported in due course.

Materials and Methods

Database Mining and Ligand Preparation. Currently, Lapatinib (**3**) is only the U.S. FDA approved HER2 tyrosine kinase inhibitor available for cancer treatment.[22] The quinazoline derivative represents a first generation HER2 targeted small-molecule anticancer agent. Two clinically used HER1 selective tyrosine kinase inhibitors gefitinib (**1**), and erlotinib (**2**) also inhibit HER2 phosphorylation and downstream signaling cascades in HER2/HER3 overexpressing cancer cells. It has been observed that most of the HER tyrosine kinase inhibitors in clinical development also show cross receptor activity. Our in-house kinase database consists of ~4500 HER2 inhibitors collected from 250 references.[23] To develop a virtual screening model targeting HER2, we have selected 474 inhibitors based on experimentally determined inhibitory activities (IC_{50} values), structural diversity, and similarity in HER2 assay conditions.[20,21,24–49] Of the 474 inhibitors, 22 compounds were included in the training set to generate pharmacophore models (Figures 1–3) The remaining 452 compounds were included in the test set to evaluate quality of the resultant pharmacophore models. HER2 inhibitory activity of these compounds was evaluated using a similar assay method. Most of the compounds are reversible HER2 inhibitors. A few irreversible HER2 inhibitors were also included in the training set based on the assumption that both reversible and irreversible inhibitors share a similar initial binding mechanism to compete with ATP for binding to HER2. Upon binding to the active site, the irreversible inhibitors form a covalent bond, which disrupts HER2 phosphorylation activity for an extended period of time.

The structures of all molecules were built in Cerius2 and minimized using open force field (OFF) methods with the steepest descent algorithm (Accelrys, Inc., San Diego).[50] A gradient convergence value of 0.001 kcal/mol/Å was used. Partial atomic charges were calculated using the Gasteiger method. The resulting geometries with partial charges were used for docking calculations and the mol files of all molecules were exported and minimized

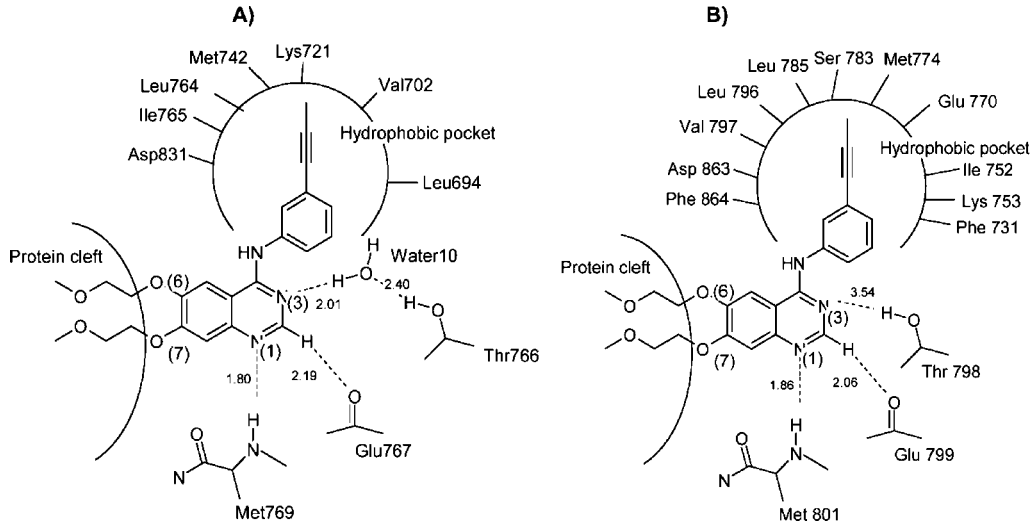

Figure 7. Bound conformation of Erlotinib inside the active site of HER1 active state (A) (1M17 PDB), and modeled HER2 active state conformation (B). The docking was carried out using GOLD.

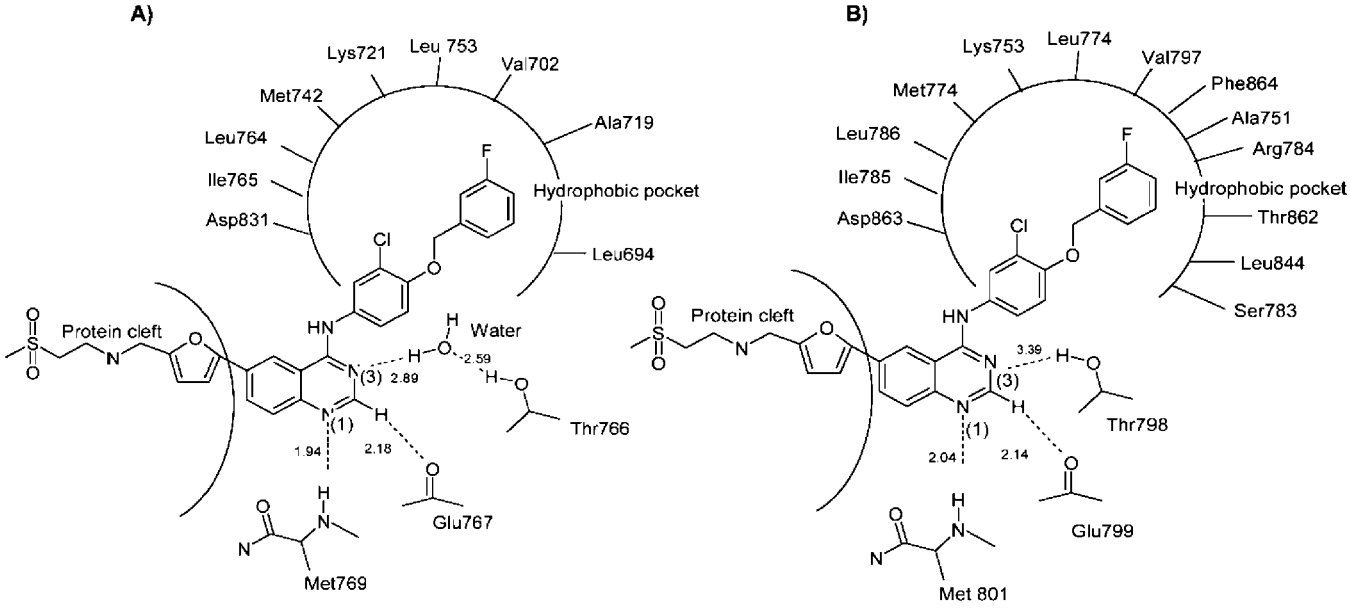

Figure 8. Bound conformation of Lapatinib inside the active site of HER1 inactive state (A) (1XKK PDB) and modeled HER2 inactive state conformation (B). The docking was carried out using GOLD.

Table 4. Observed Correlation between Docking Scores (GOLD, Glide, and eHiTS) and Experimental Activities (pIC_{50}) of the Training Set Compounds ($n = 22$)

HER2 conformation	GOLD	Glide	eHiTS
inactive state	0.844	−0.814	−0.695
active state	0.805	−0.704	−0.790

Table 5. Observed Correlation between Docking Scores (GOLD, Glide, and eHiTS) and Experimental Activities (pIC_{50}) of the Test Set Compounds ($n = 452$)

HER2 conformation	GOLD	Glide	eHiTS
inactive state	0.551	−0.596	−0.549
active state	0.545	−0.589	−0.555

using a modified CHARMM force field in Catalyst (Accelrys, Inc., San Diego).[51] Conformational analysis was carried out with the Confirm module of Catalyst. Poling algorithm of the Confirm module was employed to generate a maximum of 250 conformations for each molecule in a 20 kcal/mol energy range.[52]

Pharmacophore Model Generation and Validation. Pharmacophore modeling correlates activities with the spatial arrangement of various chemical features in a set of active analogues. A set of 474 HER2 inhibitors with an activity range (IC_{50}) spanning over 5 orders of magnitude ($pIC_{50} = 5-9$) were selected. This initial group was then divided into the training and test sets. The training set was designed to be structurally diverse with a wide activity range (Figures 1–3). The training set molecules play a critical role in the pharmacophore generation process. The quality of the resultant pharmacophore models relies solely on the training set molecules. The test set is designed to evaluate predictive ability of the resultant pharmacophore. Highly active, moderately active, and inactive compounds were added to the training set to obtain critical information on pharmacophoric requirements for HER2 inhibition. This training set was then used to generate quantitative pharmacophore models.

Qualitative pharmacophore models were generated using a set of highly active molecules (Figure 2). Common feature hypotheses (qualitative models) were produced by comparing a set of conformational models with a number of 3D configurations of chemical features shared among the training set molecules. This analysis

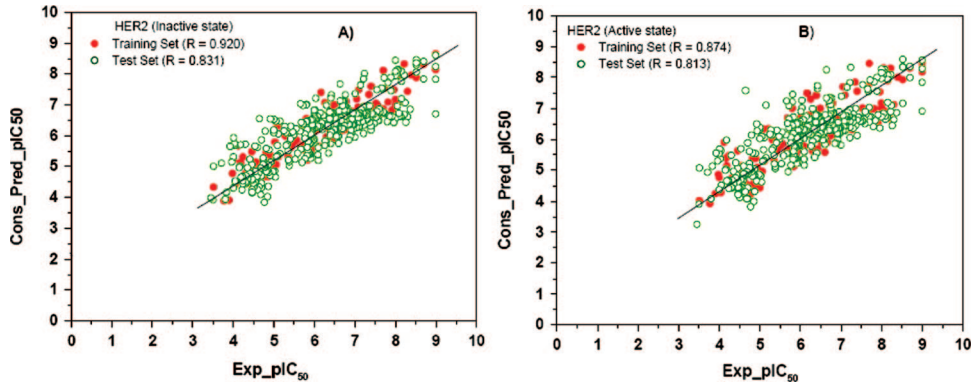

Figure 9. Scatter plots show observed correlation between experimental and HER2 inactive (A) and active (B) state consensus model predicted activities of known HER2 inhibitors.

Table 6. Validation of Consensus Models of HER2 Inactive State and HER2 Active State Conformation Using a Database of 452 Known HER2 Inhibitors

parameter	HER2 inactive state	HER2 active state
total compounds in database (*D*)	474	474
total number of actives in database (*A*)	195	195
total hits (H_t)	193	197
active hits (H_a)	156	154
% yield of actives	80.83	78.17
% ratio of actives in the hit list	80.00	78.97
enrichment factor or enhancement (*E*)	1.96	1.90
false negatives	39	41
false positives	37	43
GH score (goodness of hit)[a]	0.699	0.663

[a] GH score was calculated exactly as explained in 3.

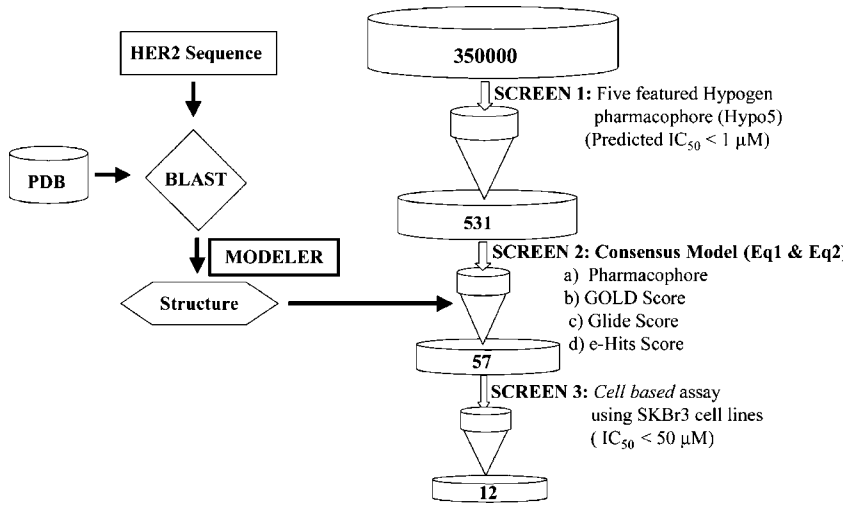

Figure 10. Schematic representation of in silico screening protocol implemented in the discovery of HER2 inhibitors.

results in a qualitative model wherein important chemical features can be easily identified. For chemically meaningful patterns, it is important to identify such chemical features before proceeding to the quantitative model generation process. To confirm essential features prevailing among the HER2 inhibitors, 10 common feature hypotheses were generated using the most active molecules **3**−**9** (Figures 1 and 2). The common features for all 10 hypotheses are HBA, HBD, and HRA. However, these models cannot be directly used to predict biological activity of the compounds retrieved from a database. We have generated quantitative pharmacophore models to predict the biological activities of novel compounds. For the quantitative model generation, 22 training set (**3**, **7**−**27**) compounds were classified as: highly active ($pIC_{50} > 6.5$), moderately active ($pIC_{50} = 6.5-5$), and inactive ($pIC_{50} < 5$). While generating the quantitative model, a minimum of 0 to a maximum of 5 features involving HBA, HBD, and HRA features were selected and used to build a series of hypotheses using a default uncertainty value of 3. In general, pharmacophore models should be statistically significant, predict the activity of molecules accurately, and retrieve active compounds from a database. The derived pharmacophore models were validated using a set of parameters including cost analysis, test set prediction, enrichment factor, and goodness of hit. HipHop and HypoGen modules within Catalyst were then used to generate qualitative pharmacophore and quantitative pharmacophore models, respectively.[51]

Modeling of Active and Inactive States of HER2 3D Structures. The HER receptors show close homology in their sequence and domain organization. They possess a ~600-residue-long extracellular region with four domains responsible for ligand binding, a single transmembrane helix, an approximately 500-residue-long intracellular region containing the conserved tyrosine kinase domain, and a less conserved regulatory C-terminal tail. To provide a molecular basis for understanding the importance of two states of HER2 conformations, we modeled active and inactive

Table 7. Cytotoxicity of Pharmacophore Hits against HER2-overexpressing SKBR3 Cell Line

Compound	Structure	Consensus model predicted HER2 inhibitory activity (IC_{50}, μM)		Cytotoxicity in HER2-overexpressing SKBR3 cell line (IC_{50}, μM)
		Eq.1	Eq.2	
28	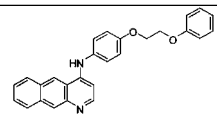	0.1	0.71	2 ± 0.2
29	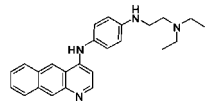	0.17	0.56	2 ± 0.2
30	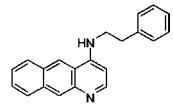	14.5	16.9	8 ± 0.3
31	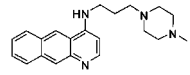	50.1	55.3	15 ± 0.4
32	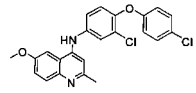	0.91	0.47	5 ± 0.1
33	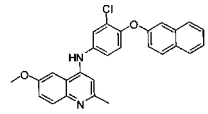	0.34	0.53	5 ± 0.2
34	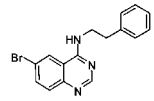	37.1	41.17	15 ± 0.5
35	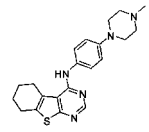	0.51	0.75	9 ± 0.5
36	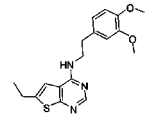	25.3	32.7	14 ± 0.5
37	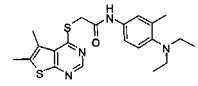	24.12	22.17	16 ± 0.3
38	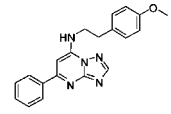	24.1	26.3	9 ± 0.5
39	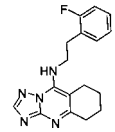	49.6	62.5	14 ± 0.4

states of the HER2 receptors based on cocrystal structures of HER1 (PDB 1M17[53]and PDB 1XKK[54]) bound to Erlotinib (**2**) and Lapatinib (**3**), respectively. The overall fold of these two crystal structures is similar, but there are significant differences in the orientation of the N- and C-terminal lobes, the C-terminal tail, and the α helix C between the lobes.[54] These orientations define the shape of the ATP binding pocket and conformation of the activation loop. In general, the N- and C-terminal lobes of kinases are connected by a flexible-hinge region. The relative orientation of these two lobes with respect to each other influences the shape of the ATP binding cleft. The 3D shape of the kinase receptor is dependent on the activation state of the kinase and the presence of their corresponding ligands. The ATP binding cleft in the HER1-Lapatinib cocrystal structure is in a relatively closed conformation. The ATP binding cleft in the HER1−Erlotinib cocrystal structure is in a more open conformation. The N-terminal lobe in the HER1−Lapatinib complex is rotated ∼12° relative to its position in HER1−Erlotinib. The magnitude of the difference suggests that these two inhibitors target different forms of the enzyme: active and inactive states. In the HER1−Lapatinib structure, residues 971−980 of the C-terminal tail form a short α helix that packs along the hinge region connecting the N- and C-terminal lobes. This helix partially blocks the front of the ATP binding cleft. A second helical segment containing residues 983−990 extends along the N-terminal lobe of the protein. The HER1−Erlotinib structure has an active activation-loop conformation. The HER1−Lapatinib structure has an inactive activation-loop like conformation.[55] On the basis of these two cocrystal structures, we modeled active and inactive states of HER2. The amino acid sequence of the HER2 kinase domain was taken from the Swissprot database (P04626). The sequence alignment was carried out using the ClustalW program to identify homologous regions between the two proteins. The catalytic domain of both HER1 and HER2 receptors is well conserved with 80% sequence identity (Figure 5). Amino acid residues Asp770 and Cys775 play a prominent role in the ATP binding pocket and confer selectivity to HER1 and HER2 inhibitors.

Modeling of the HER2 structure was carried out using the Insight II software suite (Accelrys, Inc.). Modeler algorithm was used to build models for active and inactive-like conformations of HER2. Modeler is an automated comparative modeling program designed to find the most probable structure of a protein sequence given its alignment with related structures. The model was obtained by the optimal satisfaction of spatial restraints derived from the alignment and was expressed as a probability density function for the features restrained. The optimization procedure is a variable target function method that applies a conjugate gradients algorithm to position all non-hydrogen atoms. The structure has been further refined using a molecular dynamics simulation in explicit water. The homology models of HER2 were refined by minimization using the consistent valence force field (CVFF), van der Waals cutoff of 9.5 Å, and dielectric value of $1 \times r$. Using these parameters, we performed a 1000 steps of steepest gradient followed by 1000 steps of conjugate gradient until the rms gradient was reached to less than 0.001 kcal/mol/Å. The models were embedded separately in 10 Å water layers and optimized using molecular dynamics simulation for 2 ns in 300 K temperature. The quality of the models was assessed by PROCHECK v.3.5.4 (Accelrys). Both HER2 models were evaluated by a Ramachandran plot and were compared with the topological and active site features of active and inactive-like conformations of HER1. The side chain conformations of amino acids of HER2 models (active and inactive states) were verified and found to be in a similar orientation as that of the template structures (HER1 active and inactive states).

Docking Studies. Docking calculations were performed using GOLD, Glide, and eHiTS as described below on the modeled active and inactive states of HER2. For each compound, the best 20 scored poses were collected for analysis.

1. GOLD. A collection of 474 minimized inhibitors were docked on to active and inactive states of HER2 using GOLD. A 20 Å radius active site was defined covering the ATP binding region on active and inactive states of HER2 models. Default settings for small molecule−protein docking were used throughout simulations. For each of the 10 independent genetic algorithm runs, with a selection pressure of 1.1, 100000 operations were performed on a set of 5 islands with a population size of 100 individuals. Standard operator weights were used for crossover, mutation, and migration of 95, 95, and 10, respectively. Cut-offs values of 2.5 Å for H-bonds and 4.0 Å for van der Waals were employed. Top 20 poses were collected for each molecule. The best docked score value for each

molecule associated with a favorable binding conformation compared to the cocrystallized inhibitor was considered to correlate with biological activity.

2. Glide. During the docking process, Glide initially performs a complete systematic search of the conformation, orientation, and position of a compound in the defined binding site and eliminates unwanted poses using scoring and energy optimization. Finally the conformations were further refined via a Monte Carlo sampling. The center of a grid box was defined by the center of a dummy atom of the bound inhibitor near the hinge region of the modeled HER2 protein. The enclosing box and binding box dimensions were fixed to 14 and 10 Å, respectively. The top 20 poses were collected for each compound. Docking poses were energy minimized using the OPLS-2001 force field. The best pose was selected based on Glide score and the favorable interactions formed between the compound and amino acid residues of the HER2 active site.

3. eHiTs. eHiTS evaluates all the possible protonation states for the receptor and ligands automatically for every receptor−ligand pair. The docking method systematically covers the part of the conformational and positional search space to avoid severe steric clashes. The top 20 conformations for each compound were collected and eHiTs scores were calculated for each of the 20 binding conformations. The binding conformation with high score for each compound was selected and its score was correlated with biological activity.

Consensus Model Generation. A consensus virtual screening model was generated by combination of pharmacophore and docking models (GOLD, Glide, and eHiTS). To generate a consensus model, a multiple regression analysis was carried out using the pharmacophore predicted activity and three different predicted binding scores from GOLD, Glide, and eHiTS as descriptors (X) and experimental pIC_{50} as a dependent variable (Y).

Database Screening. The Hypo5 model was used to screen a database of 350000 compounds. The search retrieved 961 hits (0.27% of database). A set of 531 compounds with predicted IC_{50} values < 1 μM were docked onto the active and inactive state of HER2 using GOLD, Glide, and eHiTs. The pharmacophore predicted activity and docking scores from the three docking algorithms were substituted in the consensus eqs 1 and 2 and the predicted activity value for each compound was calculated. Finally, 57 active hits with predicted activity values of <100 μM were selected for an in vitro assay against the HER2-overexpressing human breast cancer SKBR3 cell line.[16–18]

Cell Culture. The SKBR3 cell line was obtained from American Type Culture Collection (Manassas, VA) and was used for cytotoxicity assays. Cells were maintained as monolayer cultures in RPMI 1640 and supplemented with 10% fetal bovine serum (Gemini-Bioproducts, Woodland, CA) and 2 mM L-glutamine at 37 °C in a humidified atmosphere of 5% CO_2. To remove the adherent cells from the flask for passaging and counting, cells were washed with PBS without calcium or magnesium, incubated with a small volume of 0.25% trypsin-EDTA solution (Sigma-Aldrich, St. Louis, MO) for 5−10 min, and washed with culture medium and centrifuged. All experiments were done using cells in exponential growth phase. A 10 mM stock solution of each compound was prepared in DMSO and stored at −80 °C. Further dilutions were freshly made in media.

Cytotoxicity Assay. Cytotoxicity was measured using a 3-(4,5-dimethylthiazol-2-yl)-2,5-diphenyltetrazolium bromide (MTT) assay. Briefly, 8000 cells were seeded in 96-well microtiter plates and allowed to attach overnight. Cells were subsequently treated with a continuous exposure to the corresponding drugs for 72 h. A MTT solution (at a final concentration of 0.3 mg/mL) was added to each well and cells were incubated for 4 h at 37 °C. After removal of the medium, DMSO was added and the absorbance was read at 570 nm. The IC_{50} values were then determined for each drug by plotting the log value of drug concentration versus percent inhibition of cell growth.

Acknowledgment. This study was supported in part by DOD Concept Award to N.N. R.G. thanks Sunita Tajne, Bikash Debnath, Srinivas Odde, and Jinxia Deng for their technical support, and Laith Q. Al-Mawsawi for critical reading of this manuscript.

Supporting Information Available: Chemical structures and cytotoxicity of inactive compounds in SKBr3 cells is shown in Table S1. This material is available free of charge via the Internet at http://pubs.acs.org.

References

(1) Schlessinger, J. Cell signaling by receptor tyrosine kinases. *Cell* **2000**, *103* (2), 211–225.
(2) Wells, A. EGF receptor. *Int. J. Biochem. Cell Biol.* **1999**, *31* (6), 637–643.
(3) Guy, P. M.; Platko, J. V.; Cantley, L. C.; Cerione, R. A.; Carraway, K. L., III. Insect cell-expressed p180erbB3 possesses an impaired tyrosine kinase activity. *Proc. Natl. Acad. Sci. U.S.A.* **1994**, *91* (17), 8132–8136.
(4) Jones, J. T.; Akita, R. W.; Sliwkowski, M. X. Binding specificities and affinities of egf domains for ErbB receptors. *FEBS Lett.* **1999**, *447* (2−3), 227–231.
(5) Cho, H. S.; Mason, K.; Ramyar, K. X.; Stanley, A. M.; Gabelli, S. B.; Denney, D. W.; Leahy, D. J. Structure of the extracellular region of HER2 alone and in complex with the Herceptin Fab. *Nature* **2003**, *421* (6924), 756–760.
(6) Garrett, T. P.; McKern, N. M.; Lou, M.; Elleman, T. C.; Adams, T. E.; Lovrecz, G. O.; Kofler, M.; Jorissen, R. N.; Nice, E. C.; Burgess, A. W.; Ward, C. W. The crystal structure of a truncated ErbB2 ectodomain reveals an active conformation, poised to interact with other ErbB receptors. *Mol. Cell* **2003**, *11* (2), 495–505.
(7) Hynes, N. E.; Lane, H. A. ERBB receptors and cancer: the complexity of targeted inhibitors. *Nat. Rev. Cancer* **2005**, *5* (5), 341–354.
(8) Moy, B.; Kirkpatrick, P.; Kar, S.; Goss, P. Lapatinib. *Nat. Rev. Drug Discovery* **2007**, *6* (6), 431–432.
(9) Reid, A.; Vidal, L.; Shaw, H.; de Bono, J. Dual inhibition of ErbB1 (EGFR/HER1) and ErbB2 (HER2/neu). *Eur. J. Cancer* **2007**, *43* (3), 481–489.
(10) Spector, N.; Xia, W.; El-Hariry, I.; Yarden, Y.; Bacus, S. HER2 therapy. Small molecule HER-2 tyrosine kinase inhibitors. *Breast Cancer Res.* **2007**, *9* (2), 205.
(11) Moro, S.; Bacilieri, M.; Deflorian, F. Combining ligand-based and structure-based drug design in the virtual screening arena. *Exp. Opin. Drug Discovery* **2007**, *2* (1), 37–49.
(12) *GOLD 1.2*; CCDC: Cambridge, UK, 2002.
(13) Aparna, V.; Rambabu, G.; Panigrahi, S. K.; Sarma, J. A.; Desiraju, G. R. Virtual screening of 4-anilinoquinazoline analogues as EGFR kinase inhibitors: importance of hydrogen bonds in the evaluation of poses and scoring functions. *J. Chem. Inf. Model.* **2005**, *45* (3), 725–738.
(14) Friesner, R. A.; Murphy, R. B.; Repasky, M. P.; Frye, L. L.; Greenwood, J. R.; Halgren, T. A.; Sanschagrin, P. C.; Mainz, D. T. Extra precision glide: docking and scoring incorporating a model of hydrophobic enclosure for protein−ligand complexes. *J. Med. Chem.* **2006**, *49* (21), 6177–6196.
(15) Zsoldos, Z.; Reid, D.; Simon, A.; Sadjad, S. B.; Johnson, A. P. eHiTS: A new fast, exhaustive flexible ligand docking system. *J. Mol. Graph. Model.* **2007**, *26* (1), 198–212.
(16) Fantin, V. R.; Berardi, M. J.; Babbe, H.; Michelman, M. V.; Manning, C. M.; Leder, P. A bifunctional targeted peptide that blocks HER-2 tyrosine kinase and disables mitochondrial function in HER-2-positive carcinoma cells. *Cancer Res.* **2005**, *65* (15), 6891–6900.
(17) Gril, B.; Vidal, M.; Assayag, F.; Poupon, M. F.; Liu, W. Q.; Garbay, C. Grb2-SH3 ligand inhibits the growth of HER2+ cancer cells and has antitumor effects in human cancer xenografts alone and in combination with docetaxel. *Int. J. Cancer* **2007**, *121* (2), 407–415.
(18) Jin, Y.; Li, H. Y.; Lin, L. P.; Tan, J.; Ding, J.; Luo, X.; Long, Y. Q. Synthesis and antitumor evaluation of novel 5-substituted-4-hydroxy-8-nitroquinazolines as EGFR signaling-targeted inhibitors. *Bioorg. Med. Chem.* **2005**, *13* (19), 5613–5622.
(19) Zhang, N.; Wu, B.; Wissner, A.; Powell, D. W.; Rabindran, S. K.; Kohler, C.; Boschelli, F. 4-Anilino-3-cyanobenzo[*g*]quinolines as kinase inhibitors. *Bioorg. Med. Chem. Lett.* **2002**, *12* (3), 423–425.
(20) Tsou, H. R.; Overbeek-Klumpers, E. G.; Hallett, W. A.; Reich, M. F.; Floyd, M. B.; Johnson, B. D.; Michalak, R. S.; Nilakantan, R.; Discafani, C.; Golas, J.; Rabindran, S. K.; Shen, R.; Shi, X.; Wang, Y. F.; Upeslacis, J.; Wissner, A. Optimization of 6,7-disubstituted-4-(arylamino)quinoline-3-carbonitriles as orally active, irreversible inhibitors of human epidermal growth factor receptor-2 kinase activity. *J. Med. Chem.* **2005**, *48* (4), 1107–1131.

(21) Hudson, A. T.; Vile, S.; Barraclough, P.; Franzmann, K.W.; McKeown, S. C.; Page, M. J., *Preparation of quinoline and quinazoline protein tyrosine kinase inhibitors.* WO 9609294 A1, 1996.
(22) Feld, R.; Sridhar, S. S.; Shepherd, F. A.; Mackay, J. A.; Evans, W. K. Use of the epidermal growth factor receptor inhibitors gefitinib and erlotinib in the treatment of non-small cell lung cancer: a systematic review. *J. Thorac. Oncol.* **2006**, *1* (4), 367–376.
(23) Kinase-Database, Informatics; GVK Biosciences Pvt. Ltd.: Balanagar, Hyderabad, India.
(24) Gazit, A.; Osherov, N.; Posner, I.; Yaish, P.; Poradosu, E.; Gilon, C.; Levitzki, A. Tyrphostins. 2. Heterocyclic and alpha-substituted benzylidenemalononitrile tyrphostins as potent inhibitors of EGF receptor and ErbB2/neu tyrosine kinases. *J. Med. Chem.* **1991**, *34* (6), 1896–1907.
(25) Singh, J.; Dobrusin, E. M.; Fry, D. W.; Haske, T.; Whitty, A.; McNamara, D. J. Structure-based design of a potent, selective, and irreversible inhibitor of the catalytic domain of the erbB receptor subfamily of protein tyrosine kinases. *J. Med. Chem.* **1997**, *40* (7), 1130–1135.
(26) Hugh, R. B.; Grant, J. K. Preparation of (anilino)quinazoline derivatives as antiproliferative agents. WO 2004093880 A1, 2004.
(27) Stuart, G. C.; Clive, M. C.; Barry, S. G.; Jane, K. S. Preparation of azolylquinazolines and related compounds as protein tyrosine kinase inhibitors. WO 9802434 A1, 1998.
(28) Mien-Chie, H.; Lisha, Z. Emodin and related compounds for sensitization of HER2/neu over-expressing cancer cells to chemotherapeutic drugs. WO 9727848 A1, 1997.
(29) Neal, R.; Scott, D. K.; Samuel, J. D.; Furzhong, F. Z.; Laura, S.; Ouathek, O. Methods and compositions using bifunctional hsp-binding derivatives for degradation and/or inhibition of HER-family tyrosine kinases and treatment of cancer. WO 2000061578 A1, 2000.
(30) Hui, C.; Aviv, G.; Peter, K. H.; Elaina, M.; Laura, K. S.; Jianming, T.; Cho, P. T. Methods and compositions using receptor tyrosine kinase inhibitors for inhibiting cell proliferative disorders, and inhibitor preparation. U.S. Patent 5789427 A, 1998.
(31) Akihiro, T.; Takenori, H.; Etsuya, M. Preparation of 2-styryl-4-(phenoxymethyl)oxazole derivatives as tyrosine kinase inhibitors. WO 2001077107 A1, 2001.
(32) Yu, M.; Etsuya, M. Preparation of aralkylazoles as tyrosine kinase inhibitors useful as antitumor agents. WO 9803505 A2, 1998.
(33) Chen, H.; Gazit, A.; Levitzki, A.; Hirth, K. P.; Mann, E.; Shawver, K. L.; Tsai, J.; Tang, P. C. Methods and compositions for inhibiting cell proliferative disorders. U.S. Patent 20020068687 A1, 2002.
(34) Peter, H. K.; Pruess, S. D.; Elaina, M.; Kay, S. L.; Gyorgi, K.; Istvan, S.; Tamas, B.; Janis, H.; Laszlo, O.; Alex, L.; Aviv, G.; Axel, U.; Reiner, L.; Fairooz, F. K.; Dennis, S.; Cho, T. P. Treatment of platelet derived growth factor-related disorders such as cancers. U.S. Patent 5958959 A, 1999.
(35) Ronghui, L.; Peter, J. C.; Steven, W.; Shenlin, H.; Stuart, E.; Robert, G.; Steve, M. Preparation of 1,2,4-triazole-3,5-diamine derivatives as kinase inhibitors. WO 2002057240 A1, 2002.
(36) Stuart, C. G.; Clive, C. M.; Barry, G. S.; Jane, S. K. Preparation of bicyclic heteroaromatic compounds as protein tyrosine kinase inhibitors. WO 9802437 A1, 1998.
(37) Stuart, C. G.; Clive, C. M.; Karl, M. S.; Sadie, V.; John, P. M.; Thomas, H. A.; Paul, B.; Witold, F. K. Preparation of heterocyclyl-substituted quinazolines as protein tyrosine kinase inhibitors. WO 9703069 A1, 1997.
(38) Garcia-Echeverria, C.; Fabbro, D. Therapeutically targeted anticancer agents: inhibitors of receptor tyrosine kinases. *Mini Rev. Med. Chem.* **2004**, *4* (3), 273–283.
(39) Bridges, A. J. Chemical inhibitors of protein kinases. *Chem. Rev.* **2001**, *101* (8), 2541–2572.
(40) Revesz, L.; Blum, E.; Di Padova, F. E.; Buhl, T.; Feifel, R.; Gram, H.; Hiestand, P.; Manning, U.; Rucklin, G. Novel p38 inhibitors with potent oral efficacy in several models of rheumatoid arthritis. *Bioorg. Med. Chem. Lett.* **2004**, *14* (13), 3595–3599.
(41) Gaul, M. D.; Guo, Y.; Affleck, K.; Cockerill, G. S.; Gilmer, T. M.; Griffin, R. J.; Guntrip, S.; Keith, B. R.; Knight, W. B.; Mullin, R. J.; Murray, D. M.; Rusnak, D. W.; Smith, K.; Tadepalli, S.; Wood, E. R.; Lackey, K. Discovery and biological evaluation of potent dual ErbB-2/EGFR tyrosine kinase inhibitors: 6-thiazolylquinazolines. *Bioorg. Med. Chem. Lett.* **2003**, *13* (4), 637–640.
(42) Borzilleri, R. M.; Zheng, X.; Qian, L.; Ellis, C.; Cai, Z. W.; Wautlet, B. S.; Mortillo, S.; Jeyaseelan, R. Sr.; Kukral, D. W.; Fura, A.; Kamath, A.; Vyas, V.; Tokarski, J. S.; Barrish, J. C.; Hunt, J. T.; Lombardo, L. J.; Fargnoli, J.; Bhide, R. S. Design, synthesis, and evaluation of orally active 4-(2,4-difluoro-5-(methoxycarbamoyl)phenylamino)pyrrolo[2,1-*f*][1,2,4]triazines as dual vascular endothelial growth factor receptor-2 and fibroblast growth factor receptor-1 inhibitors. *J. Med. Chem.* **2005**, *48* (12), 3991–4008.
(43) Llauger, L.; He, H.; Kim, J.; Aguirre, J.; Rosen, N.; Peters, U.; Davies, P.; Chiosis, G. Evaluation of 8-arylsulfanyl, 8-arylsulfoxyl, and 8-arylsulfonyl adenine derivatives as inhibitors of the heat shock protein 90. *J. Med. Chem.* **2005**, *48* (8), 2892–2905.
(44) Wissner, A.; Overbeek, E.; Reich, M. F.; Floyd, M. B.; Johnson, B. D.; Mamuya, N.; Rosfjord, E. C.; Discafani, C.; Davis, R.; Shi, X.; Rabindran, S. K.; Gruber, B. C.; Ye, F.; Hallett, W. A.; Nilakantan, R.; Shen, R.; Wang, Y. F.; Greenberger, L. M.; Tsou, H. R. Synthesis and structure-activity relationships of 6,7-disubstituted 4-anilinoquinoline-3-carbonitriles. The design of an orally active, irreversible inhibitor of the tyrosine kinase activity of the epidermal growth factor receptor (EGFR) and the human epidermal growth factor receptor-2 (HER-2). *J. Med. Chem.* **2003**, *46* (1), 49–63.
(45) Smaill, J. B.; Showalter, H. D.; Zhou, H.; Bridges, A. J.; McNamara, D. J.; Fry, D. W.; Nelson, J. M.; Sherwood, V.; Vincent, P. W.; Roberts, B. J.; Elliott, W. L.; Denny, W. A. Tyrosine kinase inhibitors. 18. 6-Substituted 4-anilinoquinazolines and 4-anilinopyrido[3,4-d]pyrimidines as soluble, irreversible inhibitors of the epidermal growth factor receptor. *J. Med. Chem.* **2001**, *44* (3), 429–440.
(46) Tsou, H. R.; Mamuya, N.; Johnson, B. D.; Reich, M. F.; Gruber, B. C.; Ye, F.; Nilakantan, R.; Shen, R.; Discafani, C.; DeBlanc, R.; Davis, R.; Koehn, F. E.; Greenberger, L. M.; Wang, Y. F.; Wissner, A. 6-Substituted-4-(3-bromophenylamino)quinazolines as putative irreversible inhibitors of the epidermal growth factor receptor (EGFR) and human epidermal growth factor receptor (HER-2) tyrosine kinases with enhanced antitumor activity. *J. Med. Chem.* **2001**, *44* (17), 2719–2734.
(47) Wells, G.; Seaton, A.; Stevens, M. F. Structural studies on bioactive compounds. 32. Oxidation of tyrphostin protein tyrosine kinase inhibitors with hypervalent iodine reagents. *J. Med. Chem.* **2000**, *43* (8), 1550–1562.
(48) Smaill, J. B.; Rewcastle, G. W.; Loo, J. A.; Greis, K. D.; Chan, O. H.; Reyner, E. L.; Lipka, E.; Showalter, H. D.; Vincent, P. W.; Elliott, W. L.; Denny, W. A. Tyrosine kinase inhibitors. 17. Irreversible inhibitors of the epidermal growth factor receptor: 4-(phenylamino)quinazoline- and 4-(phenylamino)pyrido[3,2-d]pyrimidine-6-acrylamides bearing additional solubilizing functions. *J. Med. Chem.* **2000**, *43* (7), 1380–1397.
(49) Sun, L.; Tran, N.; Tang, F.; App, H.; Hirth, P.; McMahon, G.; Tang, C. Synthesis and biological evaluations of 3-substituted indolin-2-ones: a novel class of tyrosine kinase inhibitors that exhibit selectivity toward particular receptor tyrosine kinases. *J. Med. Chem.* **1998**, *41* (14), 2588–2603.
(50) *Cerius2 4.11*; Accelrys Inc.:San Diego, CA, 2005.
(51) *Catalyst 4.11*; Accelrys Inc.:San Diego, CA, 2005.
(52) Smellient, A. T., S. L.; Towbin, P. Polings-promoting conformational variation. *J. Comput. Chem.* **1995**, *16*, 171–187.
(53) Stamos, J.; Sliwkowski, M. X.; Eigenbrot, C. Structure of the epidermal growth factor receptor kinase domain alone and in complex with a 4-anilinoquinazoline inhibitor. *J. Biol. Chem.* **2002**, *277* (48), 46265–46272.
(54) Wood, E. R.; Truesdale, A. T.; McDonald, O. B.; Yuan, D.; Hassell, A.; Dickerson, S. H.; Ellis, B.; Pennisi, C.; Horne, E.; Lackey, K.; Alligood, K. J.; Rusnak, D. W.; Gilmer, T. M.; Shewchuk, L. A unique structure for epidermal growth factor receptor bound to GW572016 (Lapatinib): relationships among protein conformation, inhibitor off-rate, and receptor activity in tumor cells. *Cancer Res.* **2004**, *64* (18), 6652–6659.
(55) Liao, J. J. Molecular recognition of protein kinase binding pockets for design of potent and selective kinase inhibitors. *J. Med. Chem.* **2007**, *50* (3), 409–424.

JM7013875